JOURNAL OF APPLIED POLYMER SCIENCE VOL. 14, PP. 1597–1613 (1970)

Studies on Melt Spinning of Nylon 6. I. Cooling and Deformation Behavior and Orientation of Nylon 6 Threadline

TOHRU ISHIBASHI, *Tsuruga Nylon Plant, Toyobo Co., Ltd., Matsushima, Tsuruga, Fukui, Japan,* KIYOSHI AOKI and TSUNEO ISHII, *Fiber Research Institute, Toyobo Co., Ltd., Honkatata, Otsu, Shiga, Japan*

Synopsis

The melt spinning of nylon 6 filament yarns was studied by measuring the filament tensions at the takeup roll, the filament temperatures $\theta(x)$, filament diameters $d(x)$, and birefringence $\Delta n(x)$ as functions of distance x from the spinneret, and by observing how the molecular orientation was affected by these differences in cooling and thinning. Results were as follows: The thinning of the filament line, $d(x)$, is affected little by the spinning temperature or by the degree of polymerization of the yarns taken up; it however depends heavily on the takeup speed V_{Tu} and the rate Q of production. Trouton viscosity $\beta(T)$ as a temperature function derived from these experiments on nylon 6 is expressed consistently by the equation $\beta \doteqdot 0.34 \exp(3250/T)$, where T is absolute temperature. Nylon 6 filaments exhibit higher Trouton viscosity values than polyester or polypropylene filaments under the same spinning temperature. Filament temperature $\theta(x)$ versus distance x agreed well with theoretical values. The speed of molecular orientation was highest in the temperature range from 120°C to 40°C (the latter being the glass transition temperature of nylon 6). Furthermore, the larger the time rate of polymer deformation and the longer the residence time of polymer in the above temperature range, the higher was the orientation of the filament yarns taken up.

INTRODUCTION

Lately many studies have been published on the melt spinning of various synthetic polymer filaments involving the measurement of physical quantities of molten polymer filament leading to theoretical investigations of fiber structure formation in melt spinning.

These studies may be classified into two groups. Group I contains those engineering studies that analyze the cooling and thinning of filament lines. Group II are those that deal with the formation of microfiber structures such as orientation and crystallization.

Studies by Ziabicki,[1] Anderson,[2] and Andrews,[3] belonging to group I above, deal with the application of heat transfer theories on the cooling of running filament, although these theoretical studies failed to demonstrate good agreement with experimental results. As to the thinning of filament lines, there is an early study by Trouton[4] that introduced the concept of

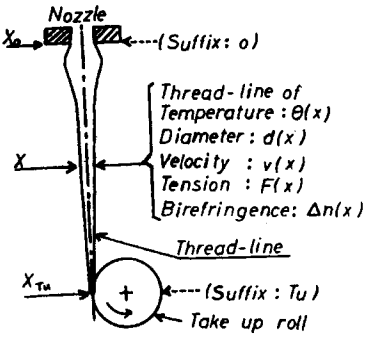

Fig. 1. Schema of melt spinning process.

Trouton viscosity (β in the present paper). Trouton, however, considered β constant in his paper. Ziabicki and Kedzierska[5] measured the diameters of thinning filaments and derived Trouton viscosities $\beta(x)$ at different distances from the spinneret. Kase and Matsuo[6–8] summarized those studies, introducing a set of simultaneous differential equations based on the heat force and material balances on the filament line, and showed that the steady state solutions of these equations for filament temperature $\theta(x)$ and cross sectional area $A(x)$ agreed well with experiments on polypropylene and polyester filaments. In order to calculate the filament diameter $d(x)$ and temperature $\theta(x)$ for the melt spinning of a given polymer it becomes necessary to know the Trouton viscosity $\beta(\theta)$ of the polymer beforehand. The $\beta(\theta)$ value should be derived from experimentally measured values in filament diameters $d(x)$ and temperatures $\theta(x)$. When the Barus effect is negligible, starting diameter d_0 may be equated to spinneret diameter. However, in most cases the maximum diameter d_{max} of the filament is so much larger than d_0 that d_{max} rather than d_0 should be used as the starting diameter. The d_{max} value is known to depend on the shape of the orifice, on the rate of production Q, and possibly on takeup speed. However, no formula known to the authors can predict d_{max} consistently. Therefore, d_{max} values had to be obtained experimentally.

As to group II studies mentioned above, Thompson[9] and Nishiumi[10] measured the birefringence Δn of running polyethylene terephthalate filament lines while in melt spinning. Chappel and associates[11] made similar measurements on nylon 66, and Nakamura[12] did the same on polyethylene, polypropylene, and polybutene-1 filaments. The only similar study on nylon 6 is by Tanimura et al.[13] on multifilament yarns under a limited spinning conditions.

In the present study we measured $d(x)$, $\theta(x)$, and F_{Tu} of running nylon 6 polybutene-filaments, and birefringence $\Delta n(x)$ of the monofilament, under various spinning conditions (see Fig. 1); derived an equation that gives Trouton viscosity β as a function of filament temperature θ; and discuss the cooling and thinning of filament lines and their influence on molecular orientation.

EXPERIMENTAL

Conditions of Experiments

Spinning draft (V_{Tu}/V_0), spinneret nozzle dimensions (0.25 mm diameter and 0.125 mm length), and takeup denier were kept constant throughout the present experiments. Three series of experiments were carried out: (1) takeup speed V_{Tu} and production rate Q were varied proportionately, (2) spinning temperature θ_0, which is the temperature of polymer melt inside the spinneret, was varied, and (3) the degree $\bar{M}_n$ of polymerization measured on yarns taken up was varied within the range of 1.85×10^4 to 2.4×10^4 (see Table I).

TABLE I
Spinning Conditions

Experiment no	$\bar{M}_n \times 10^{-4}$ [a]	Takeup velocity V_{Tu}, cm/sec	Extruding rate $Q \times 10^2$ g/sec	Polymer temperature [b] θ_0, °C
1	1.90	500	1.53	300
2	1.90	750	2.29	300
3	1.90	1000	3.05	300
4	1.90	1333	4.07	300
5	1.90	1666	5.08	300
6	1.90	2000	6.10	300
7	1.90	1000	3.05	263
8	1.90	1000	3.05	256
9	1.90	1000	3.05	242
10	2.41	867	2.64	290
11	2.35	867	2.64	290
12	2.14	867	2.64	290
13	1.85	867	2.64	290

[a] Number-average molecular weight of extruded polymer.

[b] Measured at outlet of nozzle hold ($x = 0$); diameter of nozzle, 2.5×10^{-2} cm; quench air, natural convection; diameter of filament at takeup, constant (6×10^{-4} cm); spinning way (distance from spinneret to the takeup device); 680 cm.

Measurement of Running Filament Diameter $d(x)$

A hinged tool, shown in Figure 2, is used to trap the filament as soon as it is cut with a scissors below the hinged tool. In the lower part of the spin-

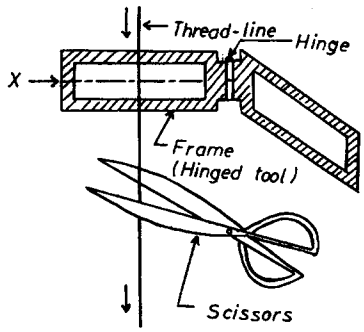

Fig. 2. Device for sampling out.

ning path where the filament was judged to have solidified, just the scissors was used to cut sample filaments off the spinning path. Cut samples were measured for their diameters under a microscope.

Measurement of Takeup Tension F_{Tu}

A tension meter having three ball-bearing rollers and using strain gauges (Strain Gauge Tension Meter Type DS6/XR by Shinko Tsushinki Co., Ltd.) was used to measure the filament tension at the takeup gadget.

Measurement of Filament Temperature $\theta(x)$

A null balance contact thermometer similar to Sasaki's[14] was fabricated by the authors to measure filament temperature. By its principle it measures the surface temperature of the filament. Since temperature gradient within the filament is estimated to be negligibly small in these experiments, measured surface temperature was assumed to represent filament temperature.

Measurement of Birefringence $\Delta n(x)$ on Running Filament

An instrument making use of the variation in the transmission of polarized light through the running filament was fabricated by the authors. It is identical in principle to Okuaki's[15] instrument developed for the measurement of Δn while fibers are heated. The running filament was placed between a pair of polarized plates.

RESULTS AND DISCUSSION

Cooling and Thinning of Filament

When Q and V_{Tu} were Varied

Figure 3 shows the different thinning of filaments when Q and V_{Tu} were varied proportionately, keeping the spinning draft V_{Tu}/V_0 unchanged. Filament diameters near the spinneret are considerably larger than the spinneret nozzle diameter of 250 μ because of the Barus effect. The larger the production rate Q, the more prominent is the Barus effect and, therefore, the larger becomes the effective spinning draft.

Figure 4 shows the measured temperature of the filament lines corresponding to the diameter curves in Figure 3. Larger production rate Q and takeup speed V_{Tu} make the temperature-versus-distance curve extend toward the right. In other words, a longer distance is required to cool the filament down to the same temperature.

In order to determine the time rates of cooling, the temperature $\theta(x)$-versus-distance x curves in Figure 4 are replotted in Figure 5 against elapsed time t after extrusion. Experiments 1, 2, and 3 in Figure 5 are fairly close together, but curves for experiments 5 and 6 for larger production rates Q extend far to the right, showing that a large production rate Q (or takeup speed V_{Tu}) brings about an actually slower cooling.

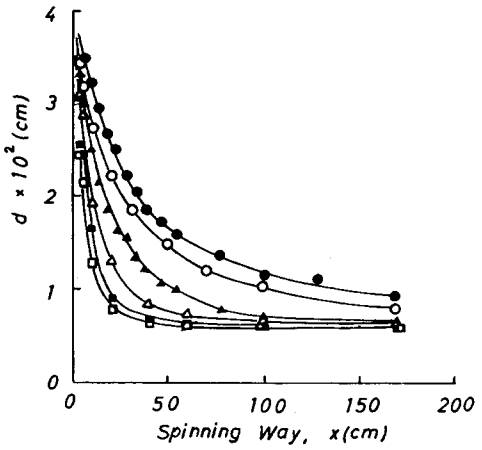

Fig. 3. Empirical diameter $d(x)$ curves for spinning condition: (□) exp. 1; (■) exp. 2; (△) exp. 3; (▲) exp. 4; (○) exp. 5; (●) exp. 6.

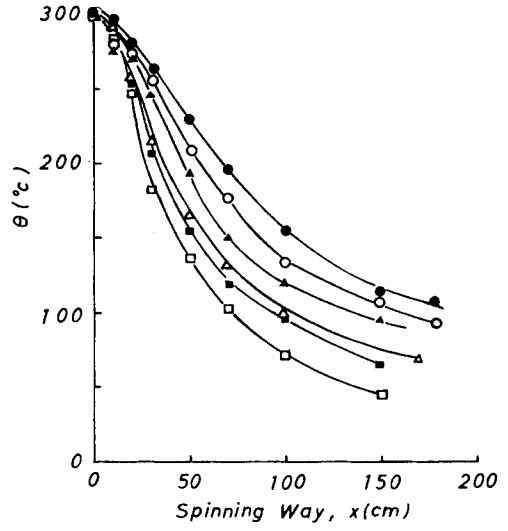

Fig. 4. Empirical $\theta(x)$ curves for spinning condition: (□) exp. 1; (■) exp. 2; (△) exp. 3; (▲) exp. 4; (○) exp. 5; (●) exp. 6.

The reason for the slow cooling at high Q is considered to be as follows. If the diameter $d(t)$-versus-time curve remains unchanged, a faster filament running speed would bring about a higher coefficient of heat transfer, resulting in a quicker cooling rather than a slower one. The primary reason why a high production rate Q resulted in a slower cooling is that a higher Q resulted in a larger filament diameter $d(t)$ below the spinneret as a result of an increasingly prominent Barus effect. More quantitative explanation is as follows. Denoting h the coefficient of heat transfer at filament surface, C_p the specific heat of polymer melt, and ρ the filament density, the tem-

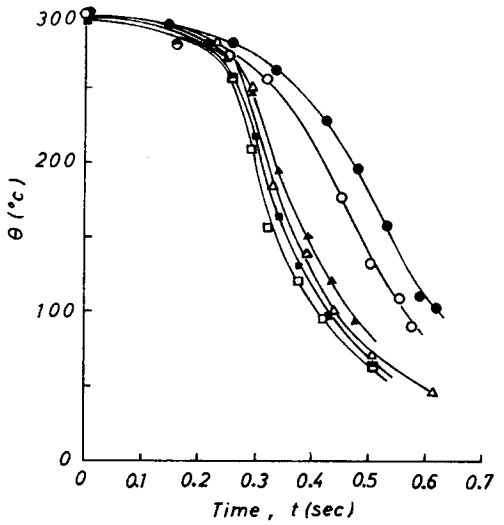

Fig. 5. Empirical $\theta(t)$ curves for spinning condition: (□) exp. 1; (■) exp. 2; (△) exp. 3; (▲) exp. 4; (○) exp. 5; (●) exp. 6.

perature of an infinitely long cylinder of uniform inside temperature surrounded by a constant temperature θ_f environment is expressed as

$$\theta(t) = \theta_f + (\theta_0 - \theta_f) \exp(-mt) \tag{1}$$

where θ_0 is the initial temperature of the cylinder and m is the cooling rate constant having the expression

$$m = -\frac{4h}{\rho C_p d} \tag{2}$$

The coefficient h of the heat transfer is given as

$$h = \frac{Nu\lambda_f}{d} \tag{3}$$

where Nu is the Nusselt number and λ_f is the heat conductivity of the surrounding atmosphere. Nusselt number Nu for a fine cylindrical body subject to air flow parallel to its axis is given by McAdams[16] as

$$Nu = 0.42\, Re^{1/3} \tag{4}$$

where Re is the Reynolds number given as $Re = dV/\nu_f$ and ν_f is the kinetic viscosity of the air. Assuming that polymer properties ρ and C_p and air properties ν_f and λ_f are constants, m in eq. (2) can be reduced to a function of diameter d and filament velocity V:

$$m = \text{const}\, d^{-5/2}\, V^{1/3} \tag{5}$$

Equation (5) shows that an increase in diameter d affects the rate of filament cooling much more than an increase in filament speed of the same

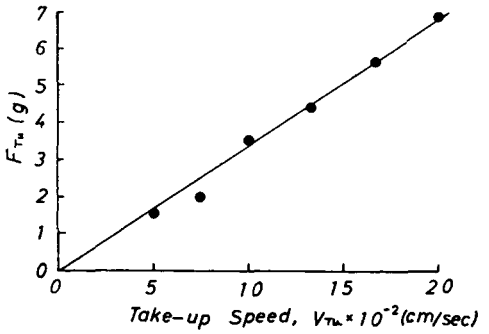

Fig. 6. Dependence of takeup tension on takeup speed.

proportion does in the reverse direction. The second reason for the slow cooling under a high production rate is that the high rate of heat discharge from the filaments raises the temperature of the ambient atmosphere.

We now would like to discuss the Trouton viscosity β, which is defined as the ratio of tensile stress $F(x)/A(x)$ and the gradient of filament speed along the filament axis; β is approximately a polymer property:

$$\frac{F(x)}{A(x)} = \beta \frac{dV(x)}{dx} \tag{6}$$

where $A(x)$ is the cross-sectional area of the filament yarn and $F(x)$ is filament tension at distance x.

Ziabicki[17] expressed $F(x)$ as

$$F(x) = F_{Tu} - \frac{Q[V_{Tu} - V(x)]}{g} + \int_x^{x_{Tu}} \rho A(x)dx - F_s(x) - F_A(x) \tag{7}$$

where g is the acceleration of gravity. The first through fifth terms on the right-hand side of eq. (7) are respectively filament tension F_{Tu} at takeup point, inertia force F_I, filament gravity F_G, surface tension F_s, and air drag force F_A.

The authors made measurements of the takeup force F_{Tu} with the results shown in Figure 6. F_{Tu} was found to be directly proportional to the takeup speed V_{Tu}. The authors derived the inertia force F_I from the measured filament diameter $d(x)$ using the relation $V(x) = 4Q/\pi\rho d^2(x)$. Gravity F_G was derived likewise from $d(x)$. Surface tension F_s was ignored as insignificant. Air drag force F_A can be expressed as

$$F_A(x) = \pi \int_0^x d(x)\tau_f(x)dx \tag{8}$$

where τ_f is the shear stress at the filament surface due to air friction. Coefficient C_f of surface friction is defined as

$$\tau_f = \frac{\rho_f V(x)}{2g} C_f \tag{9}$$

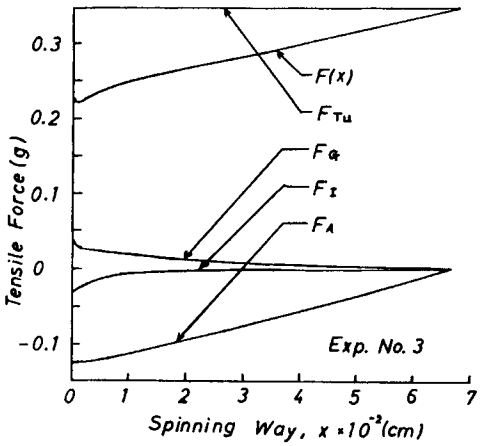

Fig. 7. Distribution of force component along the spinning way.

where ρ_f is the density of air. Ziabicki[17] computed the value of $F_A(x)$ for a takeup speed of $V_{Tu} = 656$ m/min, using eqs. (8) and (9) and a theoretical formula for C_f derived by Prandtl for a smooth infinite plane. He[17] concluded that the computed value was negligibly small in contrast to the takeup tension F_{Tu}. Kase et al. likewise ignored all tension components in eq. (7), except for takeup force F_{Tu} using $F(x) \doteqdot F_{Tu}$ as the basic assumption in their analysis of melt spinning of polypropylene[6,7] and polyester[8] fibers.

Sakiadis[18] derived theoretically an expression for the coefficient C_f of surface friction for an infinitely long cylindrical body subject to fluid flow parallel to its axis:

$$C_f = \frac{4}{B} Re = \frac{4\nu_f}{BdV} \tag{10}$$

where B is a value that satisfies

$$\frac{8\nu_f x}{Vd^2} = \int_0^B \left(\frac{Be^{2B} - e^{2B}}{B^2} + \frac{1}{B} + \frac{1}{B^2} \right) dB.$$

The authors used eqs. (8), (9), and (10) above to compute the air drag force $F_A(x)$. Figures 7 and 8 show computed contributions of each force component in eq. (7) for the conditions of experiments 3 and 6, respectively. As these figures show, air drag force F_A is too big to be safely ignored. Early calculations[17] that used the formula for an infinite plane seem to have underestimated the F_A value. Inertia force F_I, too, becomes too big to be ignored as takeup speed V_{Tu} increases.

Figure 9 shows the correlation between Trouton viscosity β and the inverse of absolute temperature T. The plotted data are those of experiments 1 through 6. The $\beta(x)$ values were derived from $F(x)$ and $V(x)$ values as discussed before and temperatures are the measured values shown in

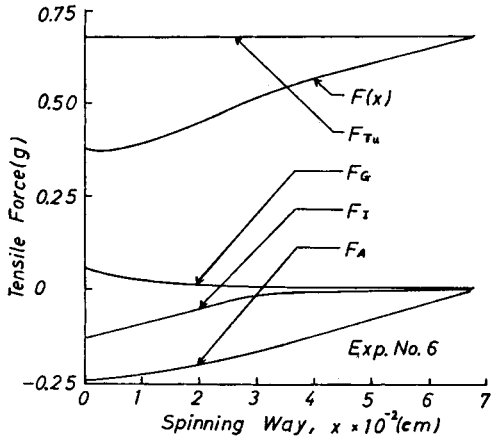

Fig. 8. Distribution of force component along the spinning way.

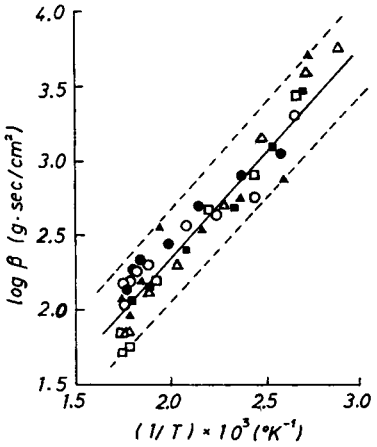

Fig. 9. Temperature dependence of Trouton viscosity: (□) exp. 1; (■) exp. 2; (△) exp. 3; (▲) exp. 4; (○) exp. 5; (●) exp. 6.

Figures 4 and 5. Although there is some scattering of data, β is related to T by the formula

$$\beta \doteqdot 0.34 \exp\left(\frac{3250}{T}\right) \tag{11}$$

over the temperature range of 250°C–80°C independent of other spinning conditions.

Comparison of Measured Values of $\theta(x)$ to Computed Values

Cooling of an infinitely long cylinder is expressed by eq. (1), which becomes

$$\theta(x) = \theta_f + (\theta_0 - \theta_f) \exp\left(-\frac{4h}{\rho C_p dV}\right)x \tag{12}$$

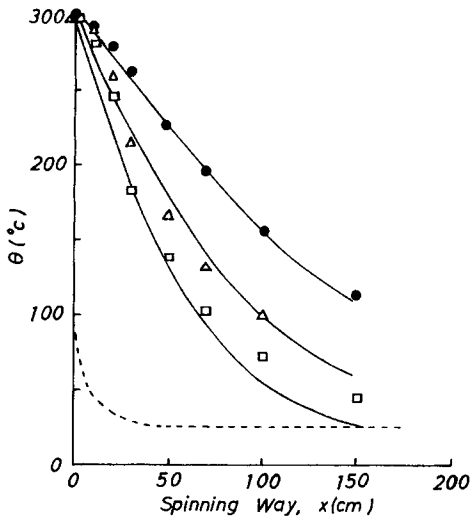

Fig. 10. Comparison of empirical with calculated value of θ(x): (□) exp. 1; (△) exp. 3; (●) exp. 6; (—) calculated curve; (- - - -) empirical temperature of environment $\theta_f(x)$ for exp. 3.

when time t is converted to distance x from the origin (spinneret). Equations (1) and (12) are correct only when θ_f, h, ρ, d, and V are constants, which is not the case in melt spinning. Since it is not easy to solve for $\theta(x)$ when above parameters are variables, the authors divided the spinning path in small increments of distances Δx so that within each increment the parameters can be regarded as constants.

Average temperature θn of nth increment Δx_n is

$$\theta_n = \bar{\theta}_{fn} + (\theta_{n-1} - \theta_{fn}) \exp\left(-\frac{4\bar{h}_n}{\bar{\rho}_n \bar{C}_{p_n} \bar{V}_n \bar{d}_n}\right)\Delta x_n \qquad (13)$$

In the actual computation, measured values of $\bar{\theta}_f$, $\bar{V}_n$, and $\bar{d}_n$ were used. In estimating the air properties ν_f and λ_f needed in computing heat transfer coefficient $\bar{h}_n$, air temperature in the boundary layer was assumed to be equal to the average of initial segment temperature θ_{n-1} and ambient temperature θ_{fn}. Filament temperatures computed in this manner are shown in Figure 10 as three curves showing a fairly good agreement with the experimental values plotted.

When Spinning Temperature θ_0 and Molecular Weight $\bar{M}_n$ are Varied

Figures 11 and 12 show measured $\theta(x)$ and $d(x)$ values for four different spinning temperature θ_0 values. While a decrease in θ_0 shifted the $\theta(x)$ curves downward, the $d(x)$ curve remained unchanged. Takeup tension F_{Tu} which fell within 0.35 ± 0.03 g was not affected appreciably by the changes in spinning temperature θ_0.

Figure 13 shows experimentally measured values of $\theta(x)$, and $d(x)$ for four different molecular weight $\bar{M}_n$ values. Evidently neither $\theta(x)$ nor

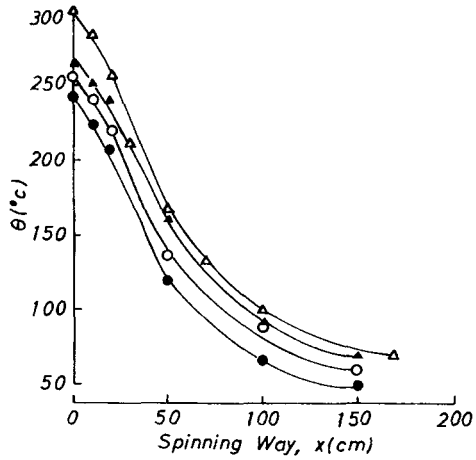

Fig. 11. Empirical $\theta(x)$ curves for various spinneret zone temperatures: (△) exp. 3; (▲) exp. 7; (○) exp. 8; (●) exp. 9.

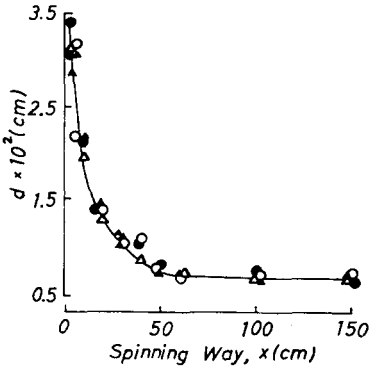

Fig. 12. Empirical $d(x)$ curves for various spinneret zone temperatures: (△) exp. 3; (▲) exp. 7; (○) exp. 8; (●) exp. 9.

$d(x)$ were affected by changes in molecular weight measured on yarns taken up. The authors, however, later conducted tests similar to the one above, changing the molecular weight $\bar{M}_n$ greatly. The test revealed that takeup tension F_{Tu} did increase with increasing molecular weight $\bar{M}_n$.[19] In other words, an increase in $\bar{M}_n$ did increase the Trouton viscosity β. In the experiments shown in Figures 11, 12, and 13 the effect of $\bar{M}_n$ was likely to be obscured by measurement errors.

In Figure 14, Trouton viscosity β derived from present experiments are plotted against the inverse of measured absolute temperature T. All the β values measured under different molecular weight $\bar{M}_n$, production rates Q, and takeup speeds V_{Tu} fell within the comparatively narrow region bounded by the two parallel dotted lines. Trouton viscosity β, therefore, may be considered for practical purposes independent of spinning conditions other than temperature T.

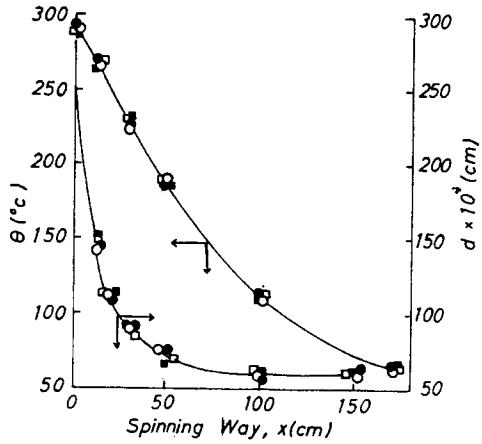

Fig. 13. Empirical $\theta(x)$ and $d(x)$ curves for polymer having various number-average molecular weights $\bar{M}_n$: (●) exp. 10; (■) exp. 11; (○) exp. 12; (□) exp. 13.

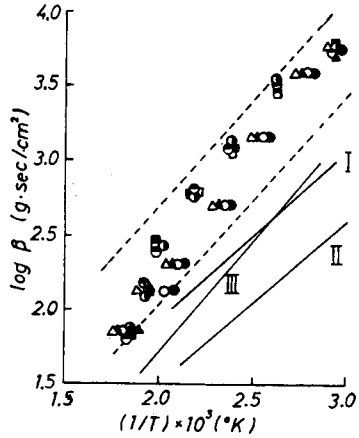

Fig. 14. Temperature dependence of Trouton viscosity on molecular weight $\bar{M}_n$: (△) exp. 3; (▲) exp. 7; (○) exp. 8; (●) exp. 9; (□) exp. 10; (■) exp. 11; (◑) exp. 12; (◓) exp. 13; solid lines I and II, polypropylene date[6,7]; solid line III, polyester data.[8]

Equation (11) derived from Figure 14 may be considered to represent in general the temperature dependence of Trouton viscosity β in nylon 6. Shown in Figure 14 in addition to the above are Trouton viscosity $\beta(1/T)$ measured by Kase et al. in their melt spinning of polyester[8] and polypropylene[6,7] filament yarns. Trouton viscosity β is the tensile viscosity defined under a velocity gradient different from that for the usual melt viscosity. It is, therefore, interesting to observe how the three commercial polymers, nylon, polyester, and polypropylene, behave with respect to the above two viscosities. Polypropylene[20] and polyester[21] have been reported to have much higher melt viscosities than nylon within the commercial range of molecular weight. The reverse was observed with Trouton

viscosity β shown in Figure 14. Furthermore, melt viscosity of nylon 6 melt spun at 250°C spinning temperature is known to be at most 1000 poises (approximately 1 g sec/cm^2) in magnitude. The Trouton viscosities β obtained in the present experiments on nylon 6, however, are more than 10 times as large as the above 1000 poises, even when the difference in velocity gradient definition is taken into consideration.

In conclusion, in the commercial melt spinning of nylon 6 filament yarns, thinning $d(x)$ and cooling $\theta(x)$ of polymer filament are affected little by changes in molecular weight $\bar{M}_n$ or spinning temperature θ_0 but are quite sensitive to changes in production rate Q or, in other words, in takeup speed V_{Tu}. The $d(x)$ and $\theta(x)$ values are sensitive to Q largely because an increasing Q intensifies the broadening (Barus effect) of streamline immediately below the spinneret. For this reason, in order to calculate $d(x)$ and $\theta(x)$ theoretically, simply substituting the Trouton viscosity formula, eq. (11), into the simultaneous differential equations given by Kase and Matsuo[6] is not enough. In addition, there must be a mathematical formula that gives the extent of the Barus effect, namely a formula that gives the starting diameter d_0 as a function of Q, orifice dimension, etc.

Molecular Orientation

Figure 15 shows the Δn values of running nylon 6 filaments measured by means of the transmission of polarized light through the filaments plotted against distance from the spinneret. Measurements were made under different takeup speeds V_{Tu}. In Figure 16, the same Δn values and speed gradients are plotted against measured filament temperatures.

Figure 15 shows that increased takeup speed V_{Tu} resulted in an increase in Δn_{Tu} at the takeup. Figure 16 shows further that increase in Δn while melt spinning takes place mostly in the temperature range 120°C–40°C, making the Δn-versus-temperature curve start to level off approximately at the glass transition point of nylon 6. Time rate of change in Δn while filament is cooled and drawn in melt spinning is given by Ziabicki,[22] Nishiumi,[10] and others as the balance between the molecular orientation due to thinning and the molecular relaxation due to thermal movement:

$$\frac{d\Delta n}{dt} = A(\theta)\left(\frac{dV}{dx}\right) - \frac{\Delta n}{\tau(\theta)} \tag{14}$$

where $A(\theta)$ above is an optical constant and $\tau(\theta)$ is the relaxation time. The resultant speed $d\Delta n/dt$ of molecular orientation while subject to cooling and thinning becomes highest in the temperature range 120°C–40°C with nylon 6. In melt spinning, the longer the polymer stays in this temperature range and the greater the rate of thinning there, the larger becomes the speed $d\Delta n/dt$ of orientation. This justifies the reasoning that a higher production rate Q (or V_{Tu}) results in a higher Δn_{Tu} at takeup because a high Q prolongs the residence time of polymer in the temperature range 120°C–40°C.

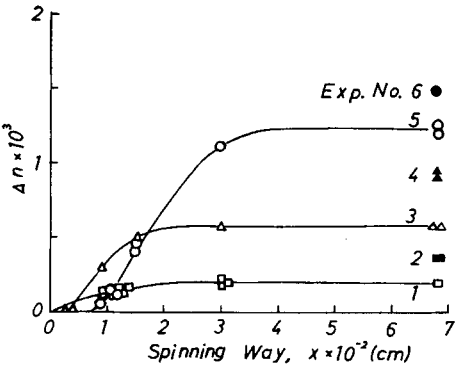

Fig. 15. Empirical Δn(x) curves for different spinning conditions (exps. 1-6).

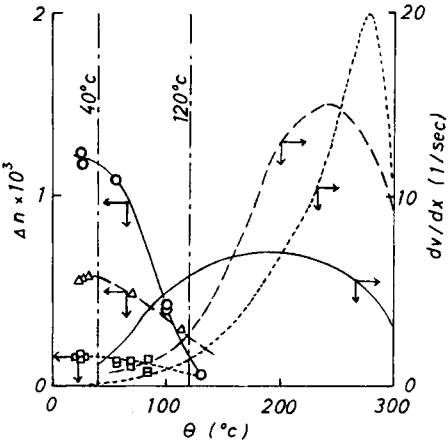

Fig. 16. Dependence of Δn on velocity gradient and temperature: (—□—) exp. 1; (- -△- -) exp. 5; (—○—) exp. 5.

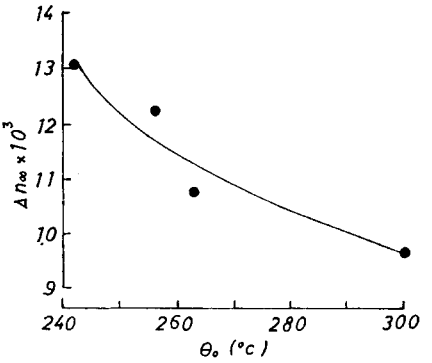

Fig. 17. Dependence of Δn_∞ on polymer temperature at spinneret.

More evidence that higher spinning temperatures reduces the Δn_{Tu} at takeup, as shown in Figure 17, can be given a similar explanation. As discussed before, changes in spinning temperature θ_0 do not affect the $d(x)$

curve appreciably. Since, the more spinning temperature θ_0 increases, the more the thinning takes place in the temperature range, the deformation to take place in the 120°C–40°C range, becomes not so large, thus reducing the Δn_{Tu} at take up.

Table II shows measured Δn_∞ values for a spinning chamber without

TABLE II
Effect of Hood Heater on Birefringence Δn_∞[a]

Heat condition	$\Delta n_\infty \times 10^3$
Normal	9.7
Heat set immediately below the nozzle	7.7
Heat set 180 cm below the nozzle	15.4

[a] Spinning condition: V_{Tu} = 1000 cm/sec, Q = 3.05×10^{-2} g/sec; cylindrical heater: 10 cm$^\phi$ × 35 cm; heat temperature: 300°C.

heater hood, with a heater hood installed immediately below the spinneret, and with a heater hood installed 180 cm below the spinneret. The Δn_∞ will be defined below. Placing a heater hood right below the spinneret is similar in effect to raising the spinning temperature θ_0. Therefore, it is reasonable that the Δn_∞ value was reduced. Installing a heater hood 180 cm below the spinneret prolongs the duration time of polymer in the 120°C –40°C range, therefore, the Δn_∞ increased as speculated beforehand.

Undrawn nylon 6 filament yarns as taken up on a melt spinning frame usually develop a considerable spontaneous extension. That is to say, filament yarns as taken in a "frozen" crystalline state tend to extend spontaneously and greatly increase Δn values when left for a prolonged time at a temperature above glass transition temperature and left to absorb moisture. Shown in Figure 18 are Δn_{Tu} values measured while in melt spinning and Δn_∞ values measured after leaving the yarn sample in a 20°C, 50% RH atmosphere so that the samples fully develop spontaneous extension. Both Δn_{Tu} and Δn_∞ are plotted against takeup speed V_{Tu}. Both Δn_{Tu}

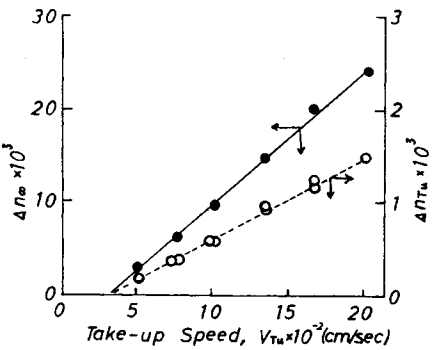

Fig. 18. Dependence of empirical (air-conditioned filaments and threadlines) birefringence on takeup speed.

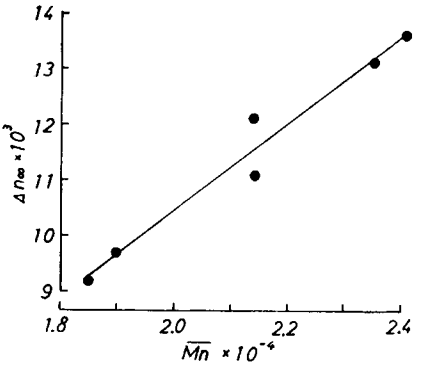

Fig. 19. Dependence of Δn_∞ on number-average molecular weight, $\bar{M}_n$.

and Δn_∞ increase linearly with takeup speed V_{Tu}, leaving a proportionality constant of about 16 between the two:

$$\Delta n_\infty \fallingdotseq 16\ \Delta n_{Tu}.$$

In Figure 19 Δn_∞ is plotted versus molecular weight $\bar{M}_n$. As discussed before, changes made in $\bar{M}_n$ within the range for usual commercial production did not affect $d(x)$, F_{Tu}, and $\theta(x)$ values to any appreciable extent. Nevertheless, Δn_∞ increases with increasing $\bar{M}_n$ as Figure 19 shows. Therefore, the speed $d\Delta n/dt$ of orientation discussed before must depend also on molecular weight $\bar{M}_n$, increasing with increasing $\bar{M}_n$. We shall report on the molecular orientation during melt spinning to greater detail in the next installment of the present study.

The studies discussed here were carried out at the Takatsuki Research Institute of the former Kureha Spinning Co., Ltd. The authors would like to express their sincerest thanks to Director E. Nagai of the Toyobo Fiber Research Institute and to Dr. O. Yoshizaki of the same institute, who have been with the authors throughout their career and have permitted to publish this paper, and to Manager K. Matsumoto of Tsuruga Nylon Plant and Chief Member S. Kase of the Toyobo Co., Ltd., for their assistance in preparing the manuscript in English.

References

1. A. Ziabicki, *Faserforsch. Textiltech.*, **8**, 467 (1957).
2. O. L. Anderson, *J. Appl. Phys.*, **29**, 9 (1958).
3. E. H. Andrews, *Brit. J. Appl. Phys.*, **10**, 39 (1959).
4. F. T. Trouton, *Proc. Roy. Soc., Ser. A*, **77**, 426 (1906).
5. A. Ziabicki and K. Kedzierska, *Kolloid-Z.*, **117**, 51 (1960).
6. S. Kase and T. Matsuo, *J. Text. Mach. Soc. Japan*, **18**, 188 (1965).
7. S. Kase and T. Matsuo, *J. Appl. Polym. Sci.*, **11**, 251 (1967).
8. S. Kase and T. Matsuo, *J. Polym. Sci. A*, **3**, 2541 (1965).
9. A. B. Thompson, *Fiber Structure*, Butterworths and The Textile Institute, Manchester and London, 1963, p. 480.
10. S. Nishiumi, *J. Text. Mach. Soc. Japan*, **18**, 174 (1965).
11. F. P. Chappel, M. F. Culpin, R. G. Gosden, and T. G. Tranter, *J. Appl. Chem.*, **14**, 12 (1964).

12. K. Nakamura, *Kogiren-Koza Text (Japan)*, 1968, pp. 4–1.
13. H. Tanimura, M. Hirami, and A. Hanawa, 17th Grand Meeting of the Society of Polymer Science, Japan, 1968, Preprint, 321.
14. N. Sasaki, *Keisoku (Japan)*, **5**, 400 (1955).
15. T. Okuaki, T. Azuma, R. Onooka, and N. Fujini, *Report of the Textile Research Institute (Japan)*, **No. 59**, 12 (1962).
16. W. H. McAdams, *Heat Transmission*, 3rd ed., McGraw-Hill, New York, 1954.
17. A. Ziabicki, *Kolloid-Z.*, **175**, 14 (1961).
18. B. C. Sakiadis, *A. I. Ch. E. J.*, **7**, 467 (1961).
19. T. Ishibashi, K. Aoki, and T. Ishii, unpublished report, 1965.
20. K. Kamiide, Y. Inamoto, and K. Ohno, *Chem. High Polym. (Japan)*, **22**, 529 (1965).
21. I. Marshall and A. Todd, *Trans. Faraday Soc.*, **49**, 67 (1953).
22. A. Ziabicki, *J. Appl. Polym. Sci.*, **2**, 24 (1959).

Received February 19, 1970.